Identification of Impurities in Synthetic Precursor Product and Metabolites of ^{177}Lu-PSMA-617 for Prostate Cancer Radiotherapy Agent Using HPLC and Tandem-Mass Spectrometry

Weihsi Chen[1*], Chuntang Chen[2], Pochih Chang[2], Shengnan Lo[2], Shihwei Lo[2] and Minghsin Li[2]

[1]Chemistry Division, Institute of Nuclear Energy Research, 1000 Wenhua Rd. Jiaan Village, Longtan District, Taoyuan City 32546, Taiwan (ROC)

[2]Isotope Application Division, Institute of Nuclear Energy Research, 1000 Wenhua Rd. Jiaan Village, Longtan District, Taoyuan City 32546, Taiwan (ROC)

*Corresponding author: Weihsi Chen, Chemistry Division, Institute of Nuclear Energy Research, Taiwan (ROC), Tel: +886-3-4711400#7200, E-mail: whchen@iner.gov.tw

Abstract

A reversed-phase high-performance liquid chromatography (HPLC) method on a Chromolith RP-18e column was employed to separate the components of a homemade PSMA-617 product. PSMA-617 is a prostate-specific membrane antigen (PSMA) inhibitor, which was labelled with radioactive nuclides, such as Lu-177, and is used as a radiopharmaceutical for the radiotherapy of prostate cancer (PC) or metastatic tumor patients. Moreover, the HPLC method was employed to study the metabolism of the active pharmaceutical ingredient (API) Lu-PSMA-617, which was incubated in the liver microsomes and kidney homogenate of rats. Impurities in the precursor PSMA-617 and the metabolites of Lu-PSMA-617 were identified via electrospray ionization triple quadrupole tandem-mass spectroscopy. The fragmentation schemes of both PSMA-617 and Lu-PSMA-617 were determined based on their tandem-mass spectra. Two impurities were detected in the homemade PSMA-617 product, of which hydrazine derivative was the major one and the other minor was the starting material. The metabolism study of Lu-PSMA-617 in the liver microsomes of rats revealed four metabolites, including Lu-PSMA-617 disintegrated into its moieties at C-N active bondings, and the metabolites lost their affinity to PC tissue or radio-emission. In the kidney, another two metabolites with the molecular weights of 494 and 696 were identified. These findings disclose the chemical and biochemical characteristics of PSMA-617/Lu-PSMA-617 and reveal a suitable way of employing radioligands.

Keywords: Lu-177-Radiotargeting Therapy; Metabolism Study; Prostate-Specific Membrane Antigen; PSMA; Radio-Theranostics

Introduction

Prostate cancer (PC) is the most common form of cancer among elderly men worldwide with high mortality [1]. Prostate-specific membrane antigen (PSMA), is a type II transmembrane glycoprotein on prostate cells surface which contain binuclear Zn^{2+} [2] active sites, and it is overexpressed in PC cells and metastatic cancers (100-1,000 fold) but has low expression density in normal tissues [3,4]. PSMA disintegrates the glutamate carboxypeptide of different substrates, such as folate hydrolysis and neuropeptide N-acetyl-aspartyl-glutamate, which are expressed in the number of organs, including prostate and kidneys [5]. PSMA has been employed as an effective diagnostic and prognostic biomarker for imaging and therapy target for PC and metastatic cancers [5,6]. Consequently, several PSMA targeting agents have been developed, including the potential candidates for clinical applications such as PSMA I&T, PSMA-10, PSMA-11, and PSMA-617 [4,6,7], which are labelled with various radio transition metals and PSMA-1007 labeled with F-18 [7]. These have been employed as radio-imaging diagnosis agents or radio-therapy medicines for metastatic or recurrent PC. The PSMA ligands have been studied with highly selective and specific antagonists of PSMA [7].

The PSMA-617 ligand was designed and developed in 2015 [8,9], which evolved from former analogs to improve its lipophilicity and affinity for PSMA and the stability of chelating with various radioactive nuclides such as Lu-177 [10], Ac-225 [10], Cu-64 [11], and Ga-68 [12], and it has demonstrated superior tumor-to-background uptake compared with previous PSMA ligands [6]. The common structural essential moiety of PSMA inhibitors includes three parts, those are glutamate-urea-lysine, chelating with transition metallic functional groups, and the spacer or linker to couple the former both. The subunit of glutamate-urea-lysine, which is a quasi-peptide bonding, is the pharmacophore that recognizes PSMA receptors [4,13] by

the oxygen of carbonyl in urea bonding to the Zn^{2+} active site [2]; therefore, it is referred to as the soul of the medicine. Substitute group derivatives in the linker modify the molecular lipophilicity, regulate the affinity to PSMA [14], and improve the tumor uptake [4]. Eighteen analogs with various configurations and the substituting groups of linkers have been synthesized to evaluate the highest potency to PSMA [2]. The study revealed that PSMA-617 is the best candidate to chelate various radionuclides and as a target vector to PSMA. In the USA, ^{177}Lu-PSMA-617 is currently under clinical trial phase III [15,16] and close to the clinical market. As a result, the precursor PSMA-617 is synthesized (the process is shown in Figure 1) [8] by the Institute of Nuclear Energy Research (INER) and labelled with Lu-177 (halflife of 6.65 days with the maximal β^- energy (E_β(max))= 497 KeV and maximal tissue penetration range of approximately 1.5 - 2 mm [17,18]) as the active pharmaceutical ingredient (API), ^{177}Lu-PSMA-617. This is primary used as a radiotherapy pharmaceutical for PC and metastatic cancer; moreover, ^{177}Lu also emits low-energy γ ray (E_γ = 208 and 113 KeV) and generates photograph on single-photon emission computed tomography (SPECT scan) to study animal models.

Even though many studies have designed lead compounds for PSMA and tested their efficacies for PC radio-imaging and therapy, the drug metabolism of PSMA inhibitors in biosystems has not been well studied yet. Drug metabolisms are related to drug safety, efficacy, and the accurate way of employing it.

Impurities in homemade PSMA-617 and the metabolites of Lu-PSMA-617 are the issues of concern in the quality of pharmaceutical and drug safety. Determining how these impurities/metabolites impact drugs in the body is required [19]. Synthesis and purification processes could be modified and quality improved depending on the identity of the impurities. The biodistribution characteristics and elimination rate
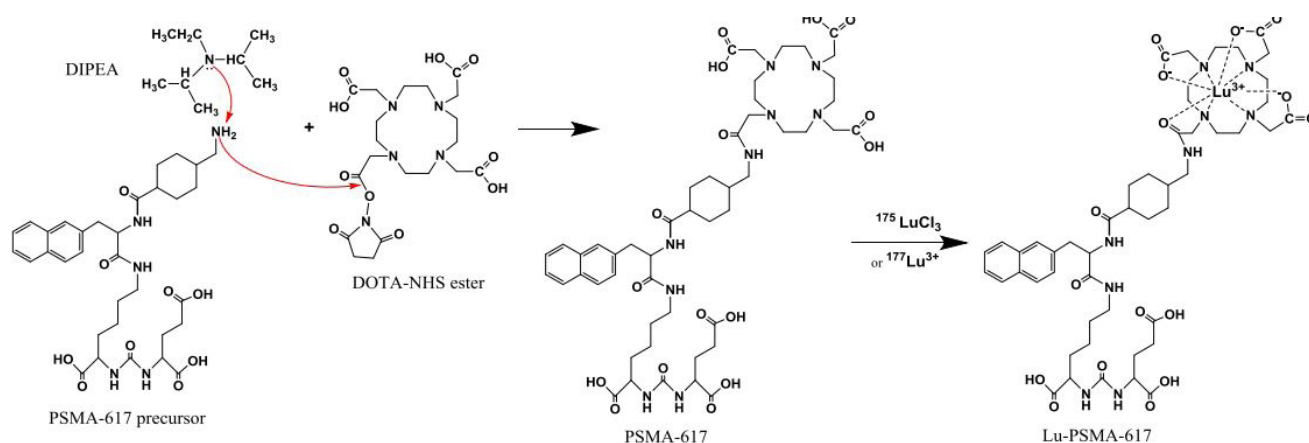
Figure 1: The synthetic scheme of PSMA-617 and drug of $^{175/177}$Lu-PSMA-617 [8].

of drugs in the body are dependent on the metabolism scheme of Lu-PSMA-617, and it is an example of the extrapolation of the biochemical behaviors of PSMA inhibitors analog imaging and therapy agents. In this study, we investigated the molecular fragmentation scheme of both PSMA-617 and [175]Lu-PSMA-617 (nonradioactive version) using electrospray ionization (ESI) triple quadrupole linear ion trap (QqQ LIT) tandem-mass spectrometry. Reversed-phase high-performance liquid chromatography (RP-HPLC) analytical method was employed to determine the PSMA-617 levels, and the impurities in PSMA-617 and the metabolites of Lu-PSMA-617 by rat liver microsomes and kidney homogenate were identified using the developed LC-MS/MS method.

Materials and Methods

Materials

The studied material, PSMA-617, was synthesized by dissolving PSMA-617 precursor peptide (purchased from Ontores, Zhejiang, China), DOTA-NHS ester (commercial from Macrocyclics, Inc., Texas, USA), and a strong base, N,N-diisopropylethylamine (DIPEA), in dimethylforamide at INER following the last step conditions reported in Ref. [8]. The PSMA-617 used as the reference standard was also purchased from Ontores. The synthesized PSMA-617 was confirmed by FT-IR, ^{1}H-NMR, and ^{13}C-NMR spectra to be identical to the purchased reference standard. Lutetium (III) chloride salt was chelated by PSMA-617 to form [175]Lu (stable isotope)-PSMA-617 complex, which was used for the metabolism study.

The liver microsomes of pooled male rats and solutions of NADPH cofactors A and B were purchased from BD Biosciences, Bedford, MA, USA. A male SD rat was sacrificed, and the pair of kidneys (2.45 g) were taken off and stored in a refrigerator at -70°C until the time for the metabolism study. Before the experiment, the pair of kidneys in a 50-mL tube was thawed in an ice bath and homogenized in 5 mL solution composed of phosphate buffer (1%, pH 7.4) solution (PBS), 0.25 M sucrose and NaCl 0.9% into total 6.5 mL of renal homogenate solution, aliquot the solution into Eppendorf tubes (1 mL per tube) and stored at -70°C.

Instruments

The components of the synthesized PSMA-617 and the Lu-PSMA-617 metabolites were separated and the levels were determined using HPLC (Agilent 1200 with online degasser, autosampler, binary pump, column oven, and diode array detector, Palo Alto, CA, USA) operated by ChemStation software, Rev. B,

0304. The detection wavelengths were set to 230 and 260 nm for the naphthalene UV absorbance. The mobile phase was a programmed gradient mixing of ammonium formate (0.32 g) and formic acid (1 mL) into 1 L aqueous solution (A pump) and formic acid 1 mL/acetonitrile 1 L (B pump) following the program: (time, min – B%) 0 – 5%, 0.2 – 10%, 3 – 30%, 6 – 60%, 9 – 95%, 10 – 95% and 10.1 – 5%, with A pump% and B pump% of 100%, flow rate of 1 mL/min, and turnaround time of 13 min per injection. The injection volume of the sample solution was 5 μL. The stationary phase was Chromolith RP18e (100 x 4.6 mm, Merck, Darmstadt, Germany) with a guard column. The components were identified based on the tandem-mass spectra data acquired by AB Sciex (Concord, ON, Canada) 4000QTRAP® mass spectrometry (equipped with electrospray ionization triple quadrupole linear ion trap, ESI-QqQ-LIT) using Analyst software 1.6.2.

Metabolism study

Hepatic metabolism study for the API was brought into [175]Lu-PSMA-617 by the male rat liver microsomes. This was performed following the protocol "Mammalian liver microsomes" guidelines for use [20]. After the incubation of Lu-PSMA-617 (250 μg mL⁻¹ in the reacted solution) with the rat liver microsomes and cofactors (NADPH A and B) for various times (5, 30, 60, 90 and 120 min), the reactions were terminated by adding 0.5 mL of iced acetonitrile (1:1), and a vortex well, which was kept in an iced-water bath, was centrifuged at 10000 x g for 10 min. The supernatant was pipetted and the solution filtered using a PVDF 0.20 μm dish filter, and the incubated solution was stored at -20 °C until the time for the HPLC and tandem-mass spectrometry. A blank sample (without Lu-PSMA-617 for background) and a control sample (50 μg mL⁻¹ Lu-PSMA-617 added to acetonitrile deactivated liver microsomes reacting system) were also prepared. For the metabolism studies in the kidney, a 0.2 mL of Lu-PSMA-617 solution (1 mg mL⁻¹ dissolved in DI water and DMSO at a ratio of 9:1) was added to 1 mL of the thawed kidney homogenate [21] mixed with a solution of the cofactor NADPH A (0.1 mL) and B (0.02 mL). After specified periods (5, 30, 60, 90 and 120 min) in a shaking thermostate water bath (37 °C), 0.2 mL of the incubated solution was taken into a microcentrifuge tube, and a 0.2 mL of iced acetonitrile was added then vortex well to stop the bioreaction. Blank and control samples of Lu-PSMA-617 in renal matrix were prepared as liver microsomes procedures. The solutions were further treated according to the steps for liver microsomes.

Results and Discussion

Tandem-mass spectra and fragmented patterns of PSMA-617 and Lu-PSMA-617

To study the structures of derivatives for PSMA-617 and Lu-PSMA-617 by tandem-mass spectrometry, the tandem-mass spectroscopy parameters were set up first by the syringe pump infusion (5 μL min⁻¹) of PSMA-617 and Lu-PSMA-617 (100 μg mL⁻¹) in ammonium formate aqueous solutions (pH 4.5) into the mass spectrometry on tuning mode. The proper mass spectrometry parameters for PSMA-617 and Lu-PSMA-617 were accessed on ramping parameters and optimized at the plateau of intensity: 15 psi of curtain gas (CUR), medium collision gas (CAD), ion-spray voltage (IS) of 5500 V, temperature (TEM) of 450 ˚C, 10 psi of both ion source gases (GS1 and GS2), declustering potential (DP) 120 - 150 V, entrance potential (EP) of 10 V, collision energy (CE) of 85 V, collision cell exit potential (CXP) of 20 V, and the interface heater was on. The representative molecular weights are 1041.5 and 1213.5 for PSMA-617 and [175]Lu-PSMA-617, respectively. The first-order MS data for PSMA-617 showed m/z of 1042.5, 1043.5, 1044.4, and 1045.4 ([M+H]⁺), 1064.5 ([M+Na]⁺), 521.8, 522.3, 522.8 ([M+2H]²⁺) (positive ion mode), and 1040.6, 1041.6, 1042.6, 1043.6 ([M-H]⁻) (negative ion mode). The MS intensity of the positive ion mode was about twenty times that of the negative ion mode for PSMA-617. Hence, the positive ion MS were collected thereafter but not the negative ion MS, except for the derivatives that might have contained a strong-acid functional group such as sulfonic acid. The first-order MS data for Lu-PSMA-617 showed m/z of 1214.5, 1215.4, 1216.4 and 1217.4 ([M+H]⁺, M = Lu³⁺-PSMA-617³⁻); 1236.5, 1237.5, 1238.5 and 1239.4 ([M+Na]⁺); 607.9, 608.3, 608.8, 609.3 ([M+2H]²⁺); and 618.8 ([M+Na+H]²⁺).

In summary, for the tandem-mass spectra of m/z = 1042 and 522 (Figure 2 (a) and (b)), the lost mass numbers from PSMA-617 included 18, 147, 173, 191, 248, 319, 347, 517, 655, 722, and 740. The fragmented structures and relationship between the m/z of the product ions for PSMA-617 are depicted in Figure 2 (c). The top three intense fragmented ion m/z were 869.5, 895.4, and 1024.6. Hence, the three ion pairs, (1042→869), (1042→895), and (1042→1024), were used as the multiple reaction monitoring (MRM) mode for the LC-MS/MS quantitative analysis of PSMA-617 in a complex matrix. In the same way, for the tandem-mass spectra of m/z = 1215 and 608 (Figure 3 (a) and (b)), the fragmentation scheme for Lu-PSMA-617 is depicted in Figure 3 (c). The lost mass numbers from the Lu-PSMA-617 molecular ion included 18, 46, 147, 173, 319, 347, 366, 435, 517, 545, etc. The broken bonding types (shown by red dashed lines) between PSMA-617 and Lu-PSMA-617 were similar, and the amide bonds [(OC)–N] were easily broken. The characteristic fragmentation patterns of PSMA-617 and Lu-PSMA-617 were the basic information for identifying unknown derivatives.
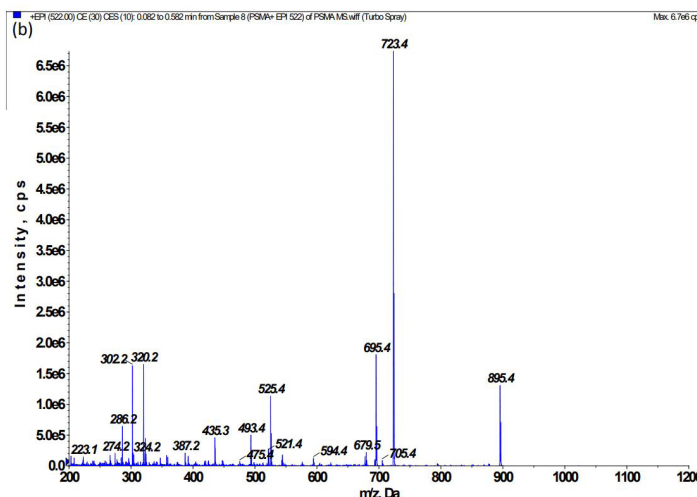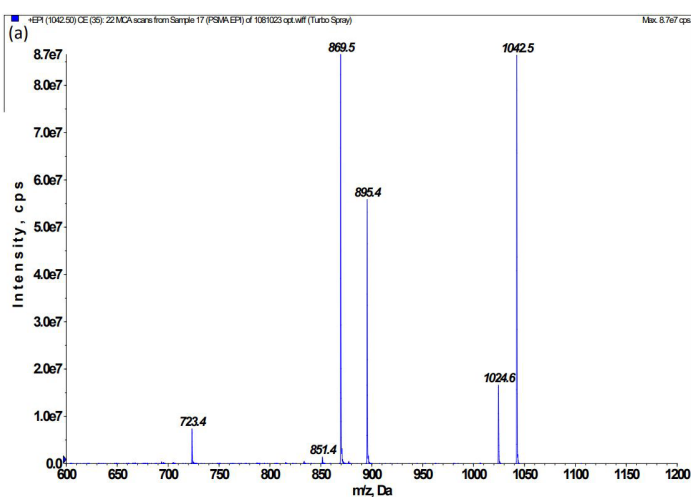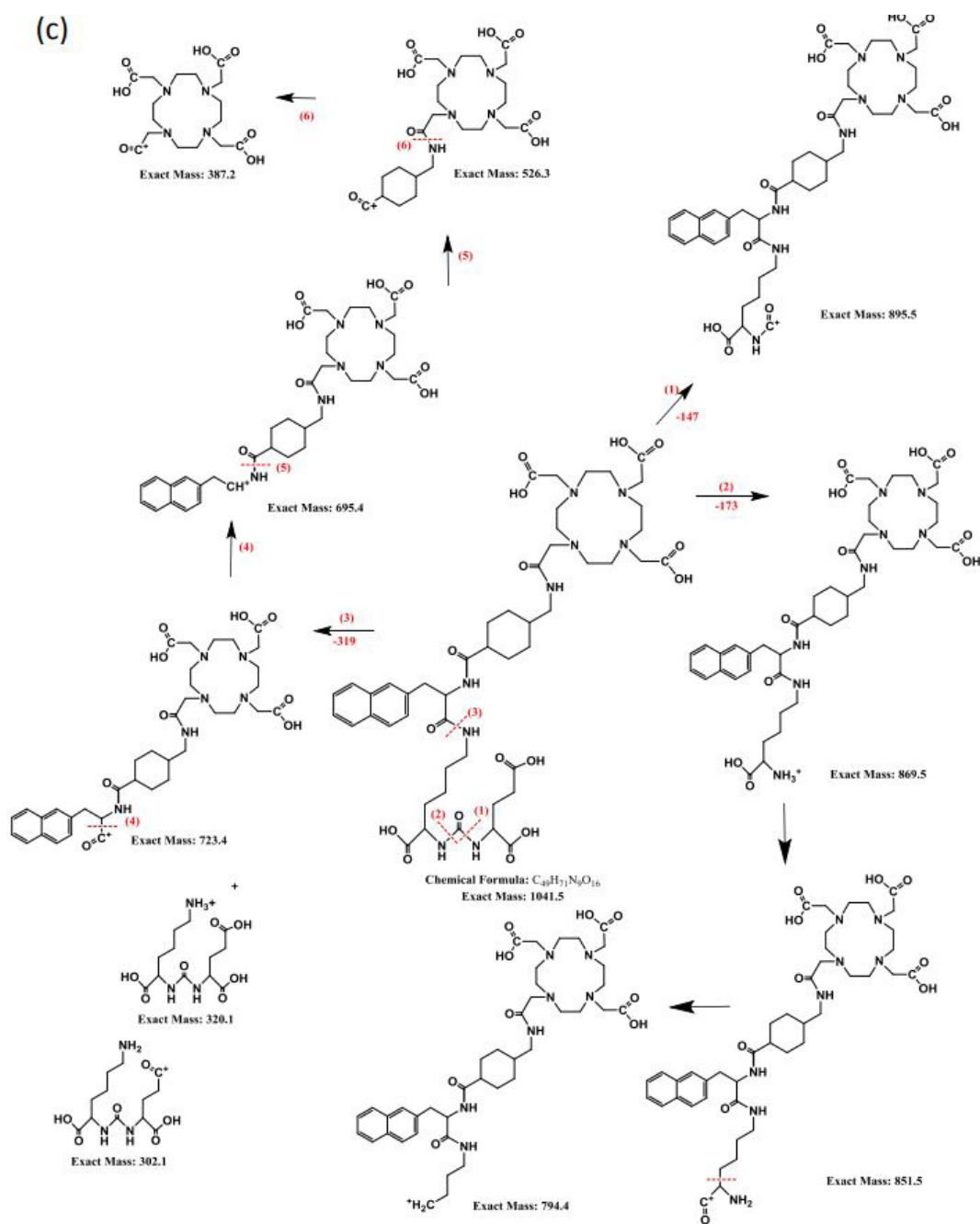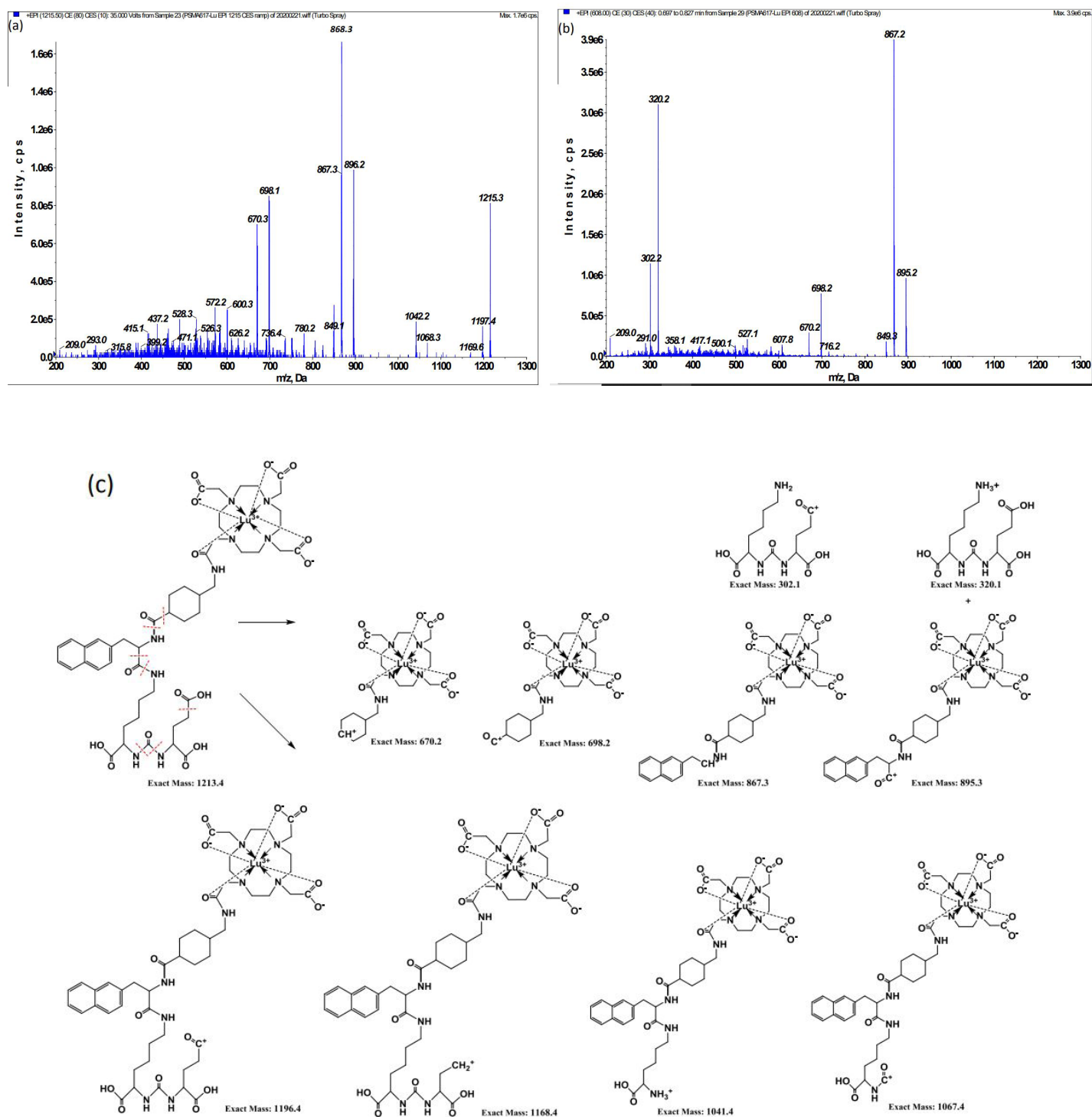
Figure 2: Tandem-mass spectra at m/z of (a) 1042 and (b) 522. (c) The fragmentation pathways of PSMA-617.

Figure 3: Tandem-mass spectra at m/z of (a) 1215 and (b) 608. (c) The fragmentation pathways of Lu-PSMA-617.

HPLC analytical method and determination of purity for synthetic PSMA-617

The RP-HPLC analytical method for PSMA-617 and Lu-PSMA-617 was run on Chromolith RP18e, a column with C18 modified single piece polymeric silica gel with meso (13 nm) and macro (2 μm) pore sizes. The pore sizes could facilitate the separation of PSMA-617 and its degraded products (size effect). The purchased PSMA-617 reference material was used as a standard to set up LC method. The detection wavelengths for PSMA-617 and Lu-PSMA-617 were 230 and 260 nm for the naphthalene absorption band. The purity of PSMA-617 in the reference material was 100%; therefore, no impurity was detected. The retention time (t_R) for PSMA-617 was 6.0 - 6.1 min with the plate number 21400. The chromatogram is shown in Figure 4 (a). The chromatographic purity of the homemade PSMA-617 product was 98.95% and two impurity peaks were observed in the chromatogram at the t_R of 5.83 and 6.35 min. The areas of the chromatographic peak were 0.2% and 0.85%, respectively (Figure 4 (b)). The t_R for Lu-PSMA-617 was 5.88 min, and the plate number was above 20000 (Figure 4 (c)). The lowest quantifiable concentration (LOQ) for PSMA617 was 5 μg mL^{-1} by UV detector (230 nm), and its linearity was better than 0.998, and the dynamic range was between 10 and 400 μg mL^{-1}.
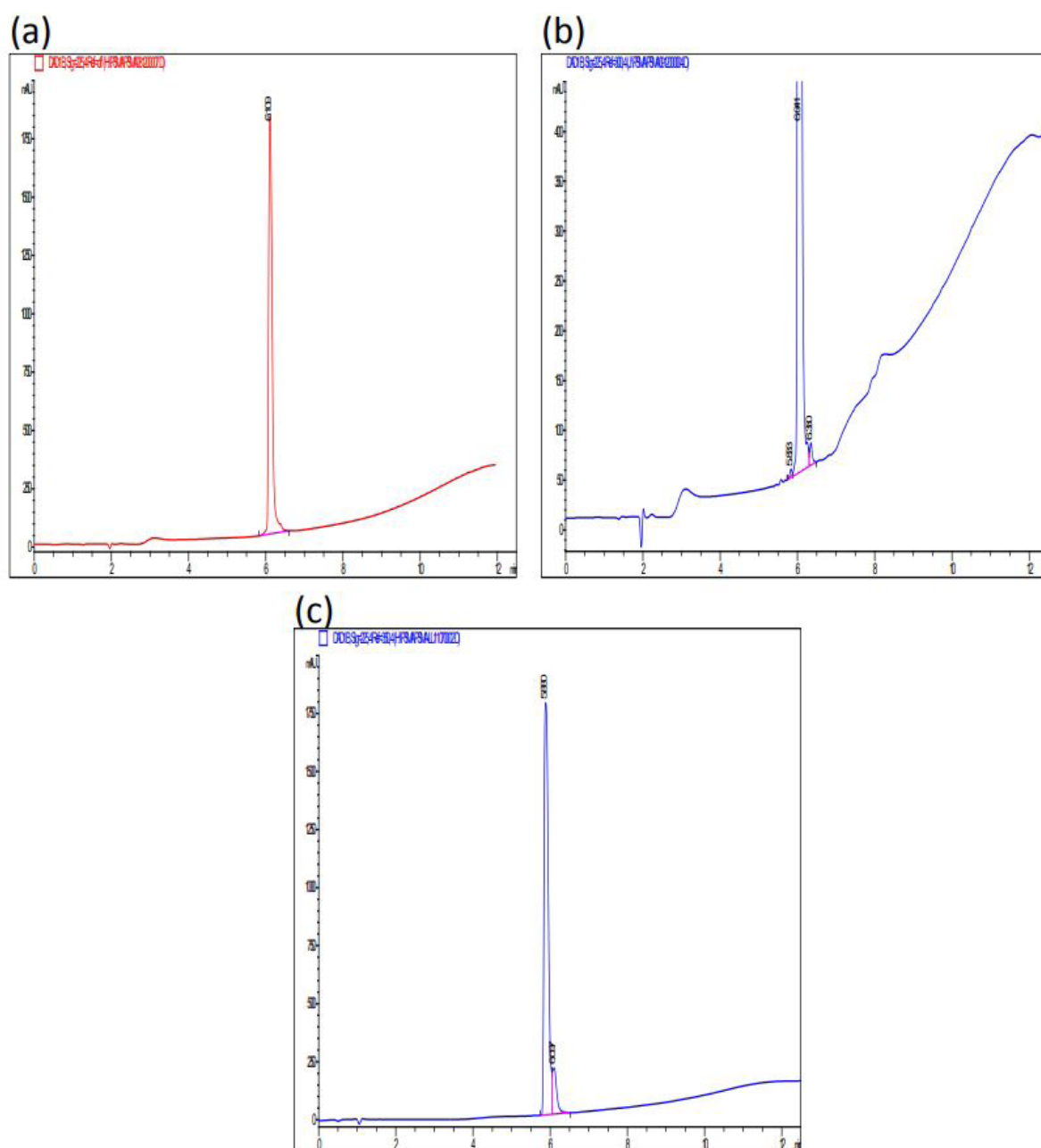

Figure 4: Chromatograms of (a) purchased PSMA-617 reference standard, (b) homemade PSMA-617 product, and (c) Lu-PSMA-617.

Determination identity of impurity in PSMA-617

The molecular and fragmented ion mass spectra of impurity peak 1 (Imp. 1) at t_R = 5.83 min for PSMA-617 show that the trace Imp. 1 was the starting material, PSMA-617 precursor with molecular ion m/z = 656 –659, the mass distribution ratio of 71:28:6:1, respectively, and the collision activated dissociation (CAD) fragmented ion mass spectra for m/z = 656 are shown in Figure 5(a). The fragmentation pathway of Imp. 1 is shown in figure 5(b), which explains the meaning of tandem-mass spectra. The molecular ion m/z for the Imp. 2 peak at t_R = 6.35 min was 1057.4 and its daughter ion mass spectra are shown in Figure 6. Similarities and differences in the data of the tandem-mass spectra between PSMA-617 and Imp. 2 are listed in Table 1 to determine the relationship between them. Based on the tandem-mass data, the identity of Imp. 2 was a hydrazine derivative of PSMA-617. The structures of the fragmentation ion of Imp. 2 are shown in Figure 7. Imp. 2 formed possibly because the N-H bond of the amide of PSMA-617 was attacked by the free pyrrolidine-2,5-dione (the product of NHS ester) to form N-N bond and then pyrrolidine-2,5-dione was hydrolyzed to form a hydrazine group. In the later synthesized batches, after repeated precipitation and LC purification, less than 0.1% of both Imp. 1 and 2 were remained.
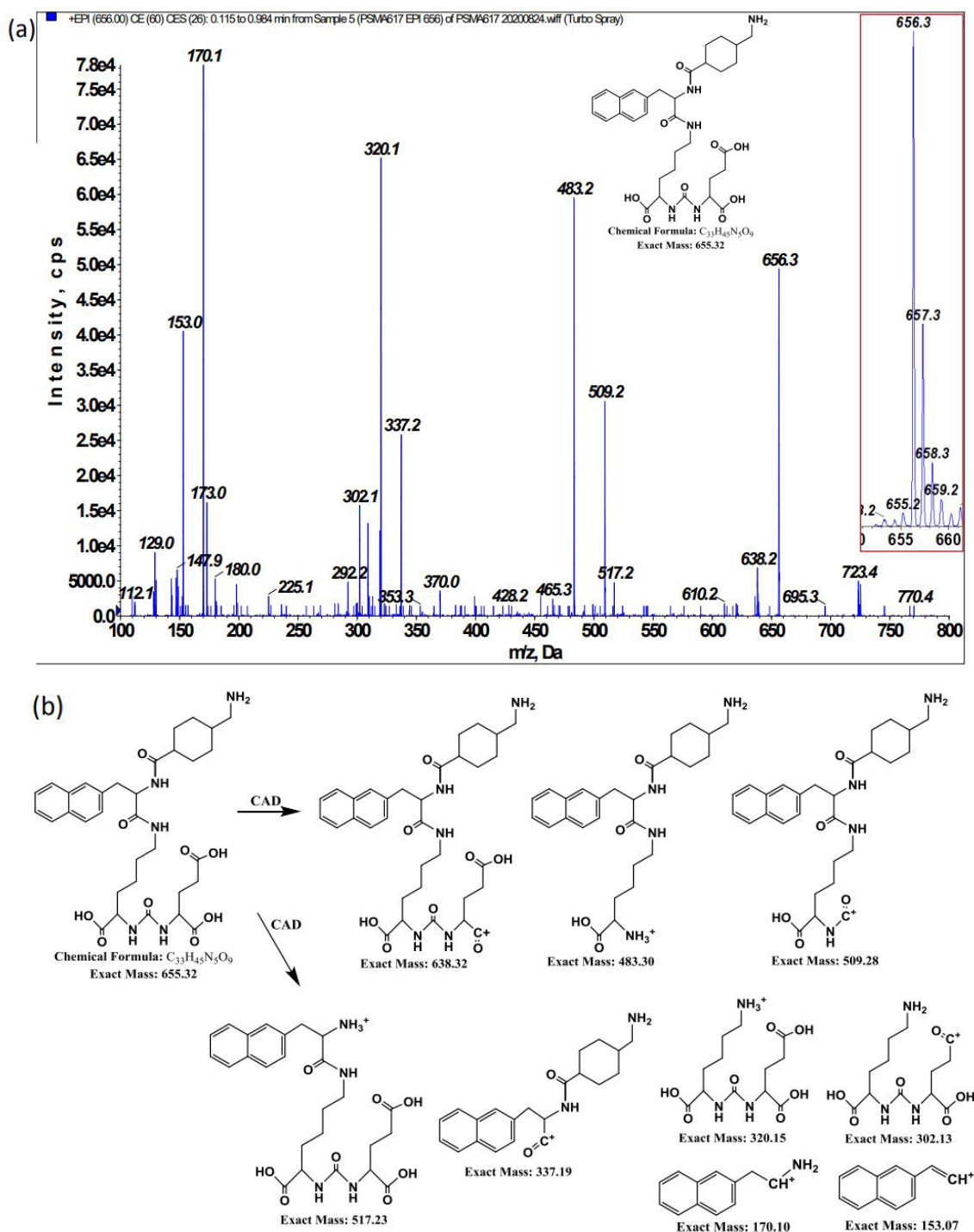
Figure 5: (a) Molecular and fragmented ion mass spectra of impurity 1 at retention time tR of 5.83 min and (b) molecular fragmentation pathway.
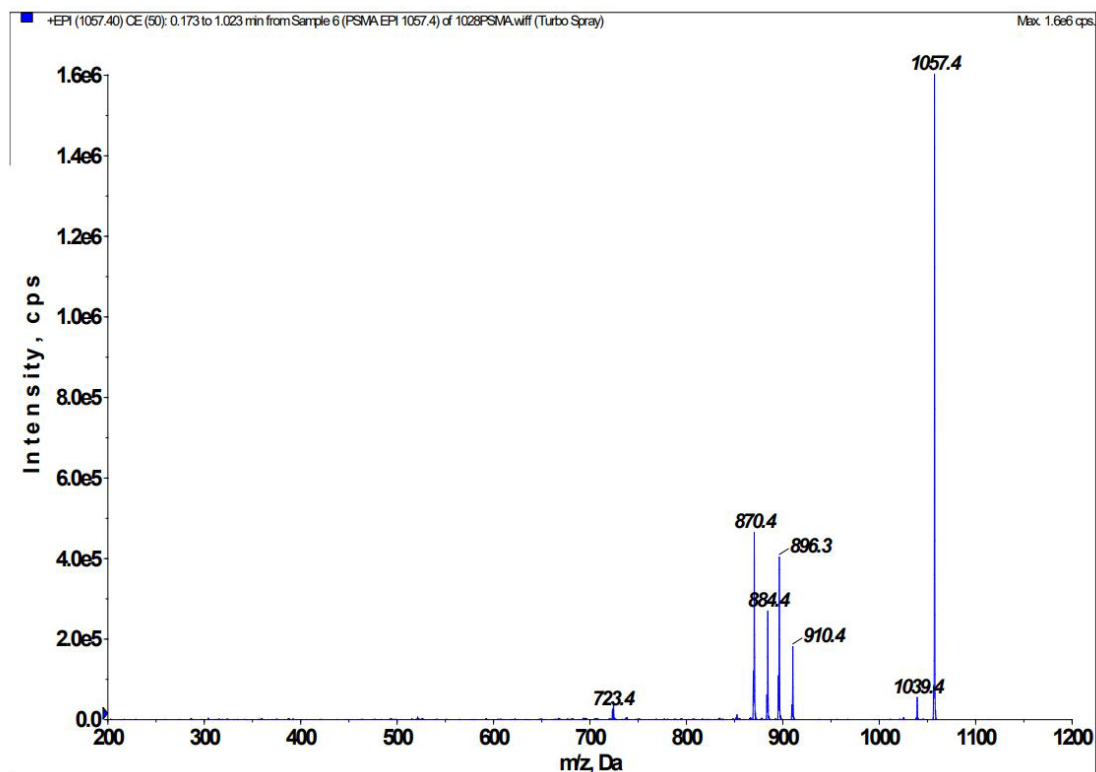
Figure 6: Tandem-mass spectra of m/z = 1057 for Impurity 2 at retention time tR of 6.35 min in PSMA-617.

	PSMA-617	Impurity 2
Molecular ion m/z	1042.3	1057 (ΔPSMA-617 = + 15) ➜ -NH ➜ -N-NH$_2$
Fragmented ion m/z	1024.4 (-18, -H$_2$O)	1039.4 (Δimpurity = -18, -H$_2$O)
	895.4 (-147)	910.4 (Δimpurity = -147) 896.3 (Δimpurity = -147-14)
	869.4 (-173)	884.4 (Δimpurity = -173) 870.4 (Δimpurity = -173-14)
	851.4 (-191)	852 (Δimpurity = -191-14)
	723.4 (-319)	723.4 (Δimpurity = -319-15)

Table 1: Comparison of the similarities and differences of tandem-mass spectra of PSMA-617 and Imp. 2.
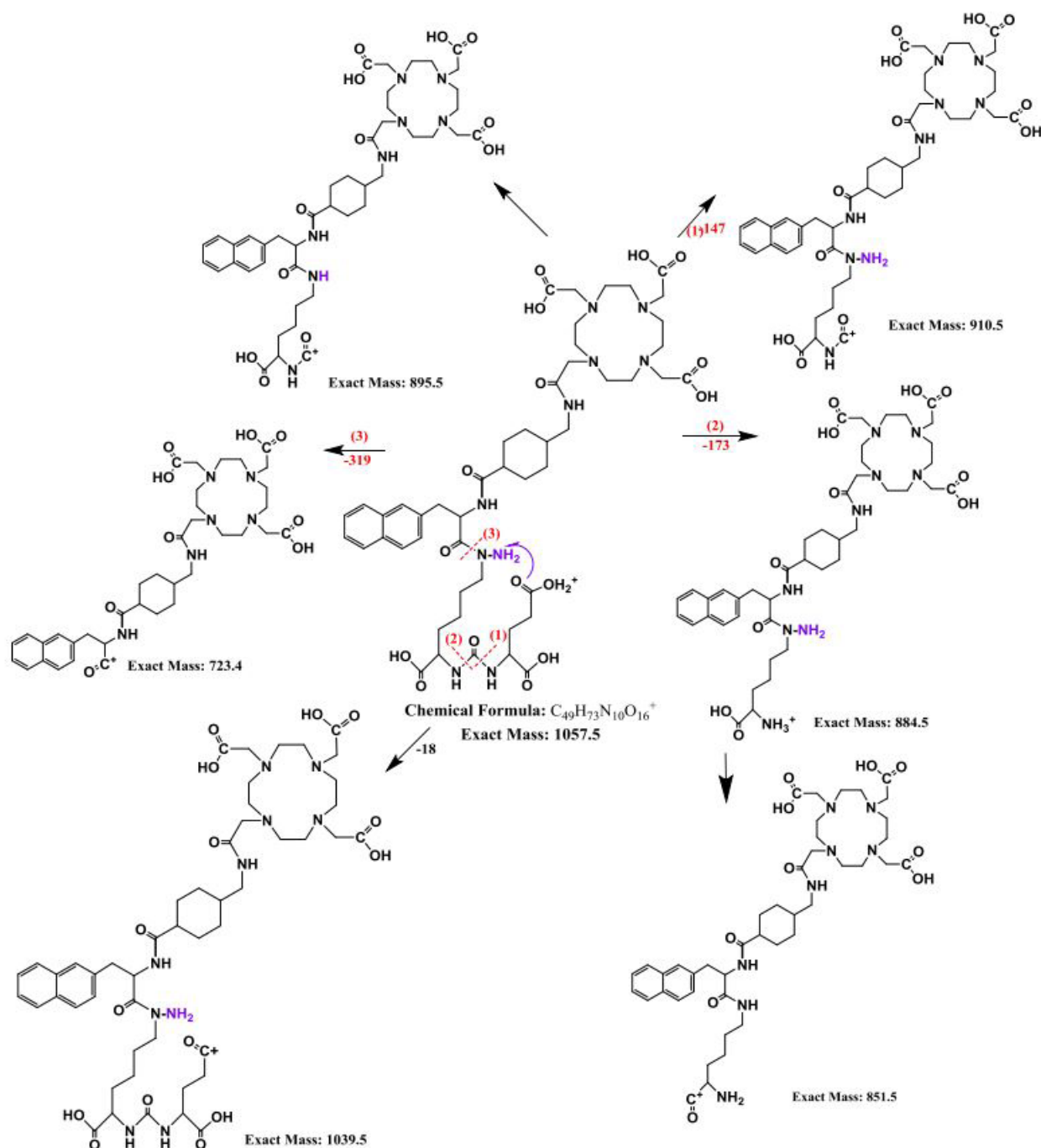
Figure 7: Supposed identity of Imp. 2 and its fragmented structures in synthetic PSMA-617 product.

Determination of Lu-PSMA-617 metabolites in rat liver microsomes

The biotransformation of xenobiotics into smaller or more hydrophilic metabolites, which leads to the deactivation, reduction of toxicity and elimination of drugs through urine or bile, is the common route for most drugs [22]. Liver accounts for the major metabolic activity, but other organs, including the kidney and enzymes in plasma, also contribute to metabolism. It is a convenient and widely accepted method to study of drug metabolism by commercial liver microsomes. In addition to this, S9 cell line, cytosol, hepatocyte, and liver homogenate solutions can also be used [23]. After incubating with the liver microsomes for the specified periods and preparing the solutions for HPLC-mass spectrometry, the potential primary m/z (MS[1]) for the metabolites were selected by comparing the ligand blank and Lu-PSMA-617 in a hepatic-enzymatic- incubated solution mass spectra and eliminating the background noise mass spectra. Four molecular ion m/z at 307, 365, 432, and 896 were observed at t_R = 2.3, 2.5, 3.4, and 5.8 min (LC-MS[1], extracted ion count, XIC mode), respectively. The fragmented ions m/z for the potential metabolites by CAD were acquired to determine their subunits and identities, as shown in Figures 8 – 11, respectively. The identified metabolites structures show that Lu-PSMA-617 inclined to disintegrate into several of its moieties at C-N active bondings, whereas higher polarity function groups, such as hydroxyl, carboxyl, and imine, were transformed. Lu nuclide was still firmly chelated by tetraaza-polyacid-macrocyclic group (because Lu^{3+} is an 8-coordinated ion [24]) in one of the metabolites (m/z at 896) but it lost the recognizing pharmacophore to PSMA receptor, glutamate-urea-lysine subunit. Conversely, the other three metabolites lost Lu and tetraaza-polyacid-macrocyclic group but preserved the pharmacophore. Consequently, these metabolites no longer had an affinity for PC cell, radio-tracability or radio-damaged for PC tissue, and they were easily eliminated from the body.
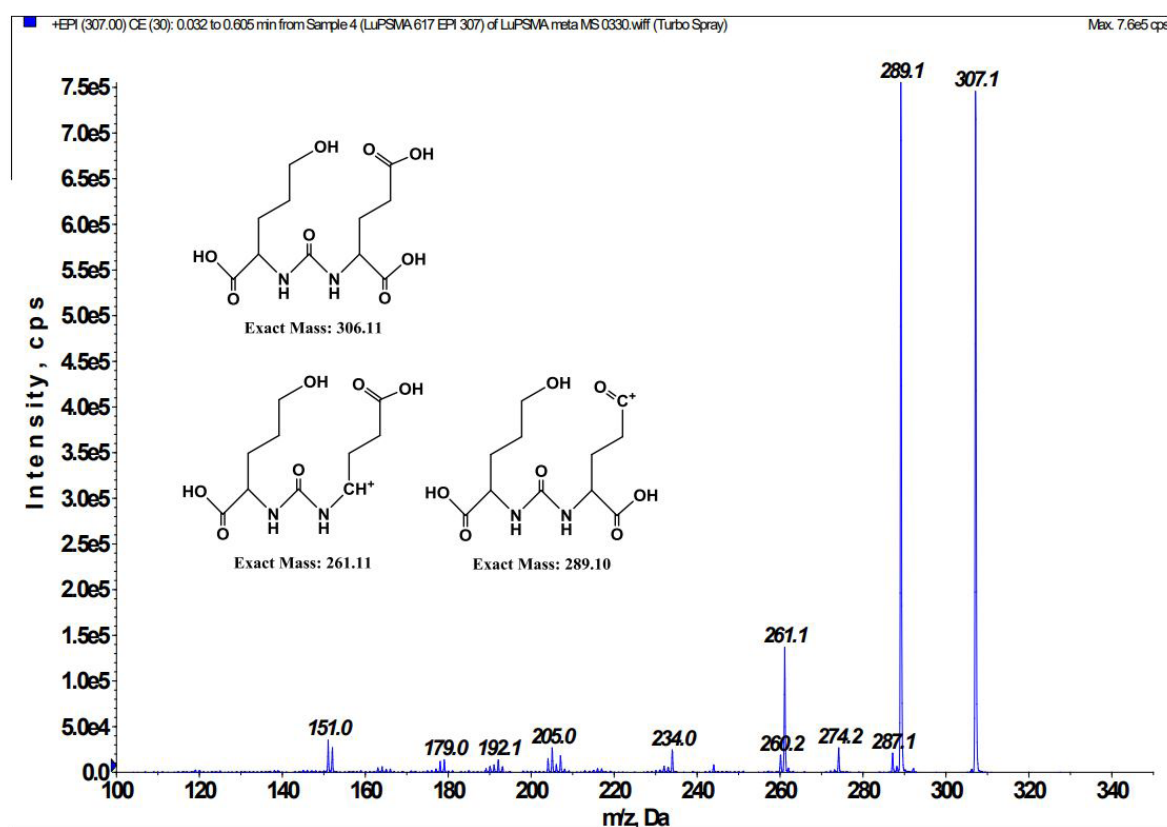

Figure 8: Fragmented ion mass spectra at m/z = 307 and supposed metabolite identity by rat liver microsomes.
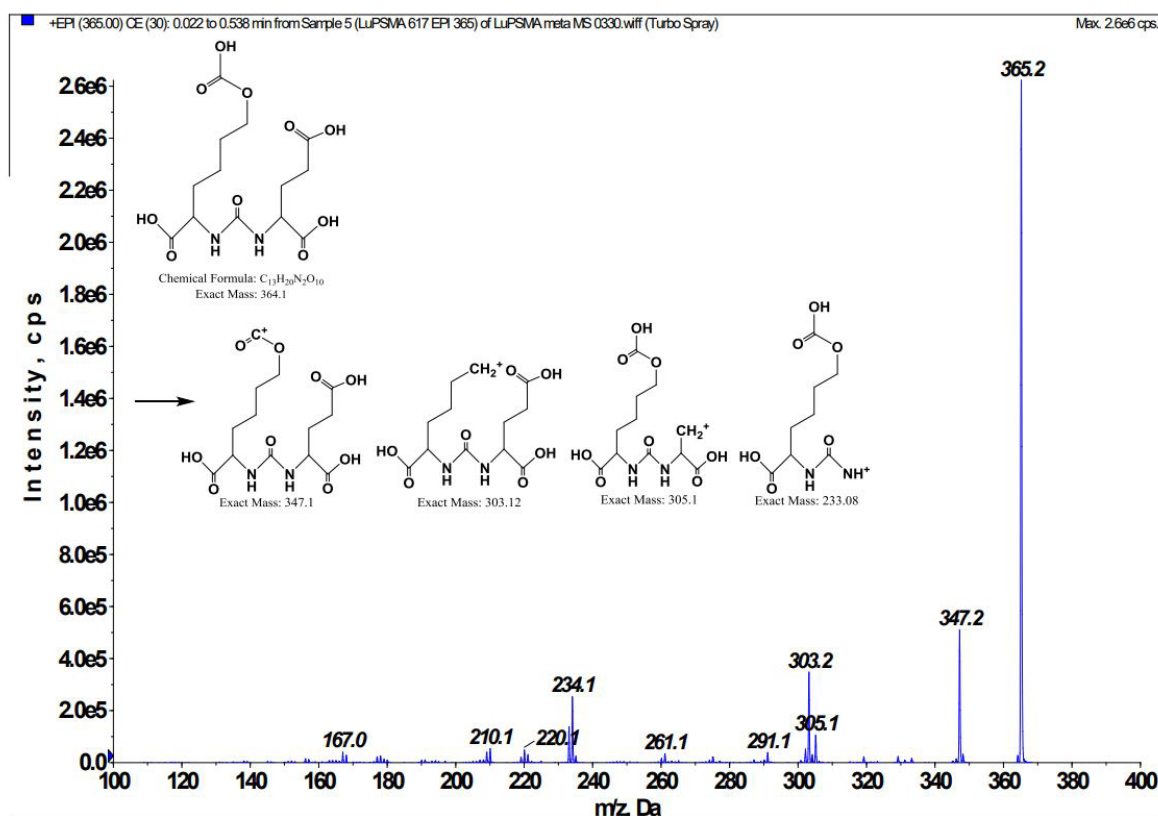
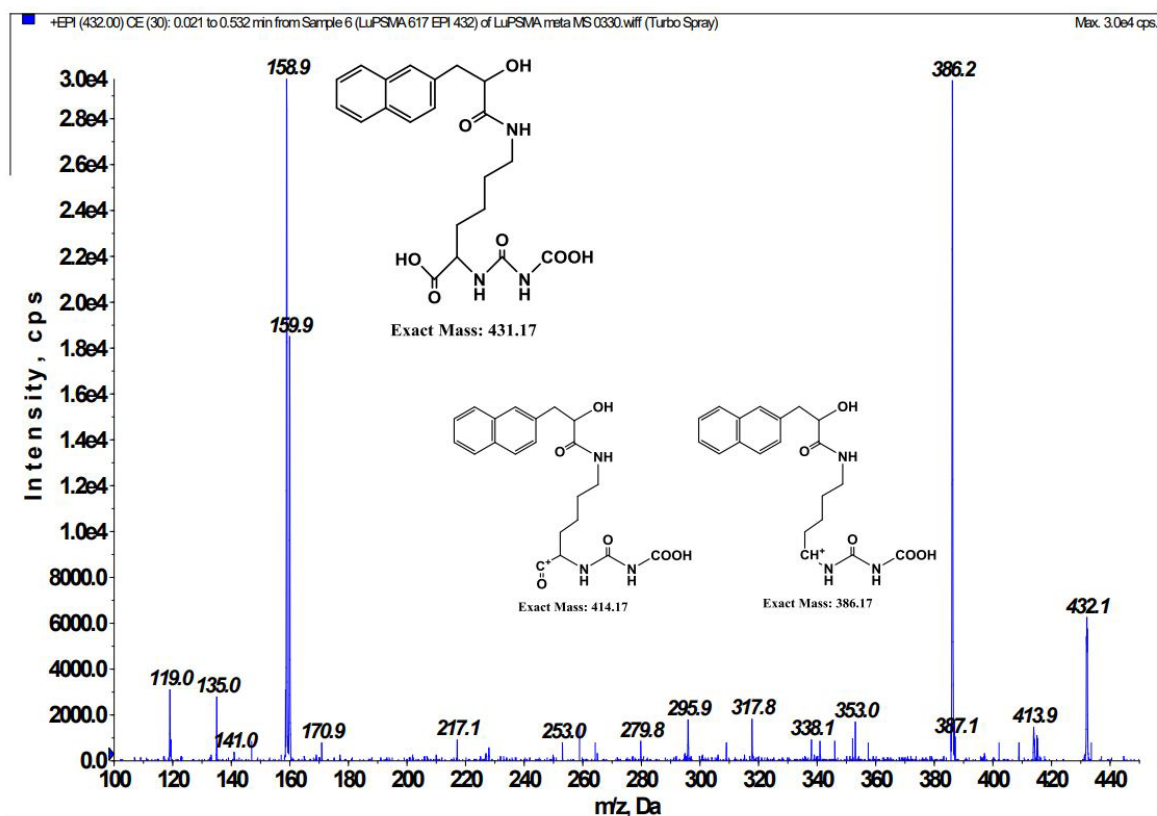**Figure 9:** Fragmented ion mass spectra at m/z = 365 and supposed metabolite identity by rat liver microsomes

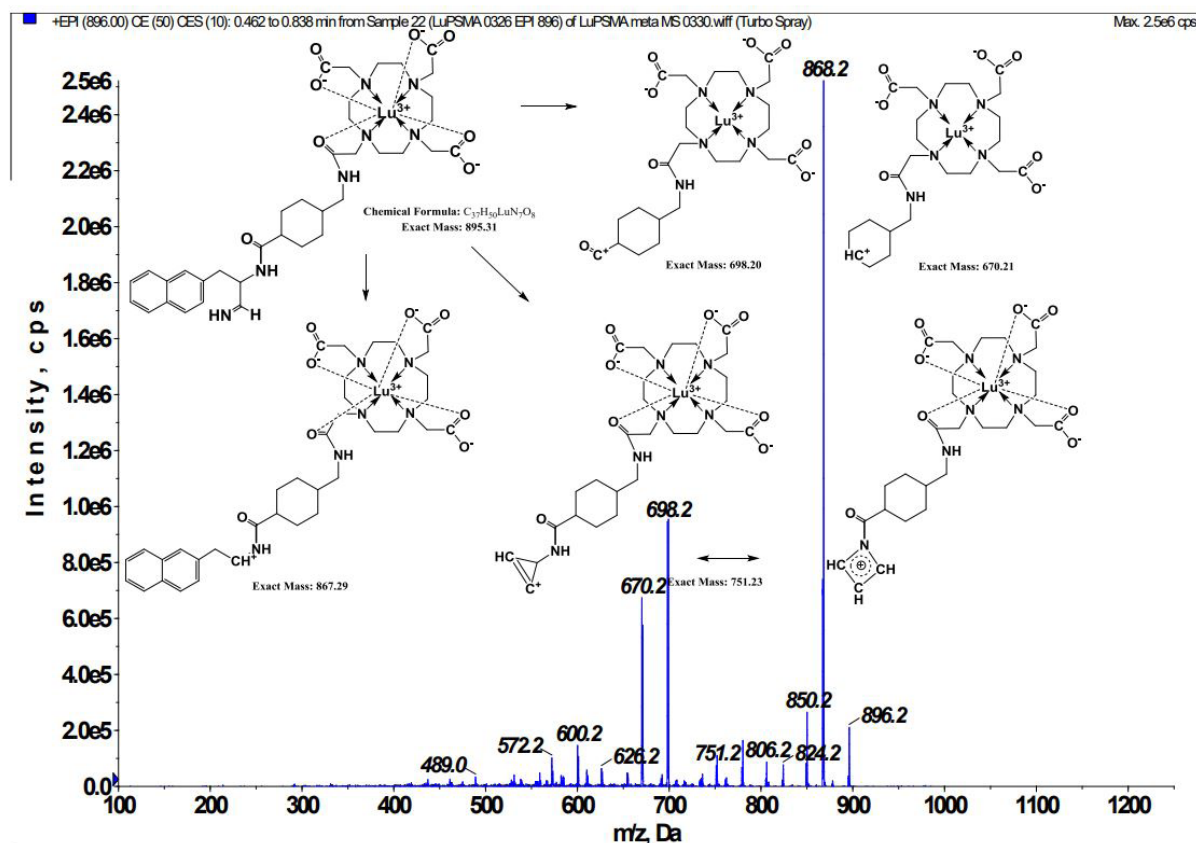**Figure 10:** Fragmented ion mass spectra at m/z = 432 and supposed metabolite identity.

Figure 11: Fragmented ion mass spectra at m/z = 896 and supposed metabolite identity.

Determination of Lu-PSMA-617 metabolites in rat kidney

Base on the ^{68}Ga-PSAM I&T image, the kidney can concentrate PSMA inhibitors at high concentrations [14], and the kidney also expresses PSMA. The function of kidney is to filter, recycle, and excrete for most chemicals through urine. Drug dosing depends largely on kidney function [25]. Compared to the liver, there are limited studies on drug metabolisms related to the kidney is really that involve the P450s and UGTs family [26]. Understanding the role of the kidney in the drug metabolism of Lu-PSMA-617 is important [27]. In the present study, we considered the metabolism of Lu-PSMA-617 in the kidney, which was implemented with a homogenate solution of rat kidneys as liver homogenate [21]. After incubating for 120 min, four metabolites of rat liver microsomes were also present in the rat kidney homogenate but at much low levels. Furthermore, two more metabolites were detected by LS-MS. One of the metabolites with the molecular ion m/z of 495 and t_R of 4.1 min was an acetamide product by the fragmented ion mass spectra, and it lost Lu-tetraa-za-polyacid-macrocyclic moiety (Figure 12). Another metabolite with m/z = 697 at t_R = 5.6 min was detected. Its fragmented ion mass spectra and the supposed structures are shown in Figure 13. Both metabolites indicate that Lu^{3+} escaped from the chelation of tetraazamacrocyclic, and Lu-PSMA-617 lost its recognition ability to PSMA in the kidney and was no more radio-theranostics efficacy.
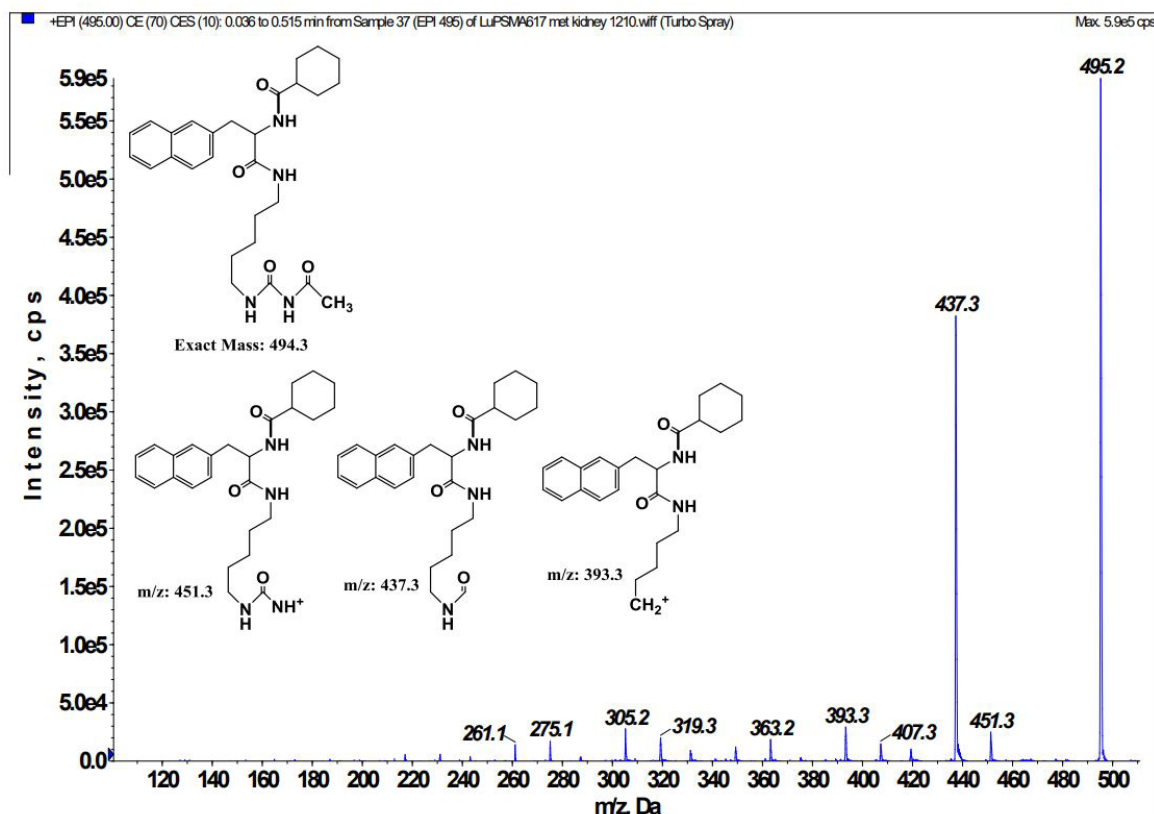
Figure 12: Fragmented ion mass spectra at m/z = 495 and supposed metabolite identity by rat kidney homogenate.
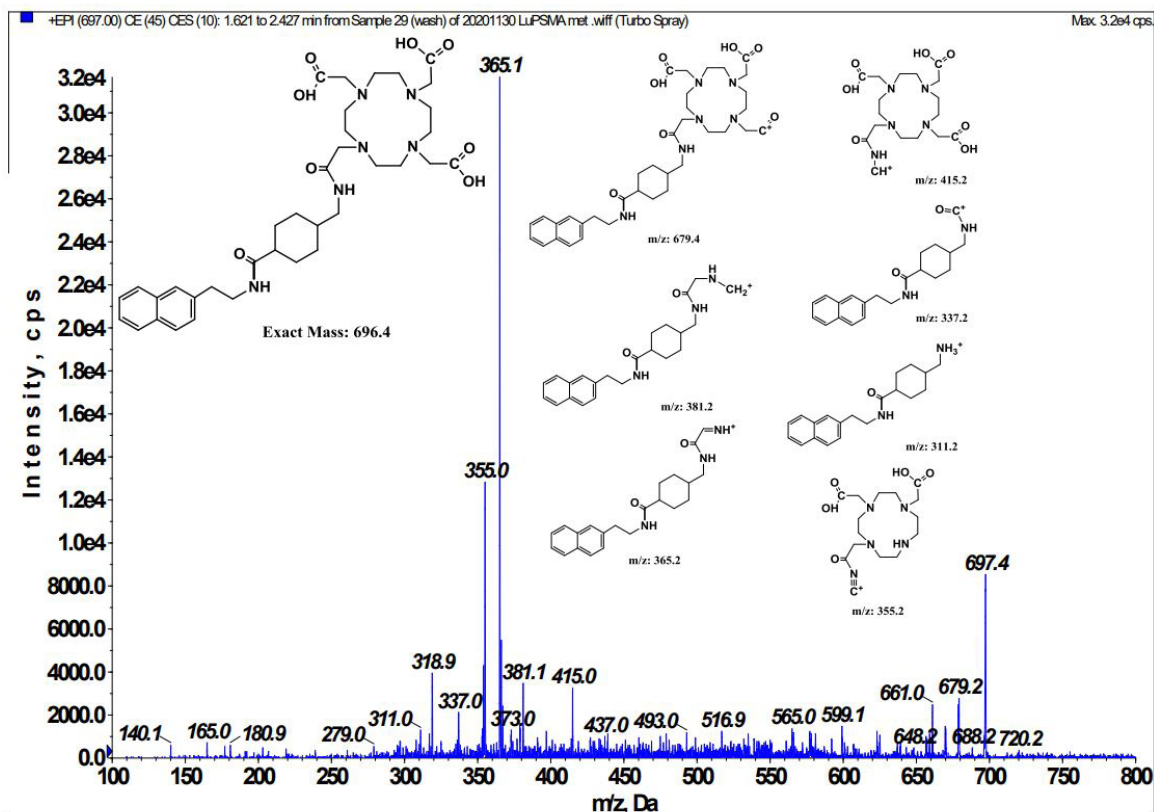

Figure 13: Fragmented ion mass spectra at m/z = 697 and supposed metabolite identity by rat kidney homogenate.

Conclusions

The fragmentation schemes and structural characteristics of a radiopharmaceutical precursor PSMA-617 and an API, Lu-PSMA-617 were elucidated, which revealed amide bondings were fragile. One of the impurities in home-made PSMA-617 was its starting material, the PSMA-617 precursor, and the other one was its hydrazine derivative. The quality of the synthesized PSMA-617 product and the reasons for the presence of impurities were qualified and improved. The metabolisms of Lu-PSMA-617 in the kidney and liver are demonstrated in Figure 14. These metabolites either lost the glutamate-urea-lysine group and the recognizing ability to PSMA or the Lu nuclide could no longer emit β- or γ rays. Therefore, the mission of the administrated ^{177}Lu-PSMA-617 radiopharmaceutical was completed and eliminated the radio-medicine. This study demonstrates the biodegradation mechanism of Lu-PSMA-617 and informs one to plan the dosage and frequency for administering ^{177}Lu-PSMA-617 to PC patients and managing their excrements.
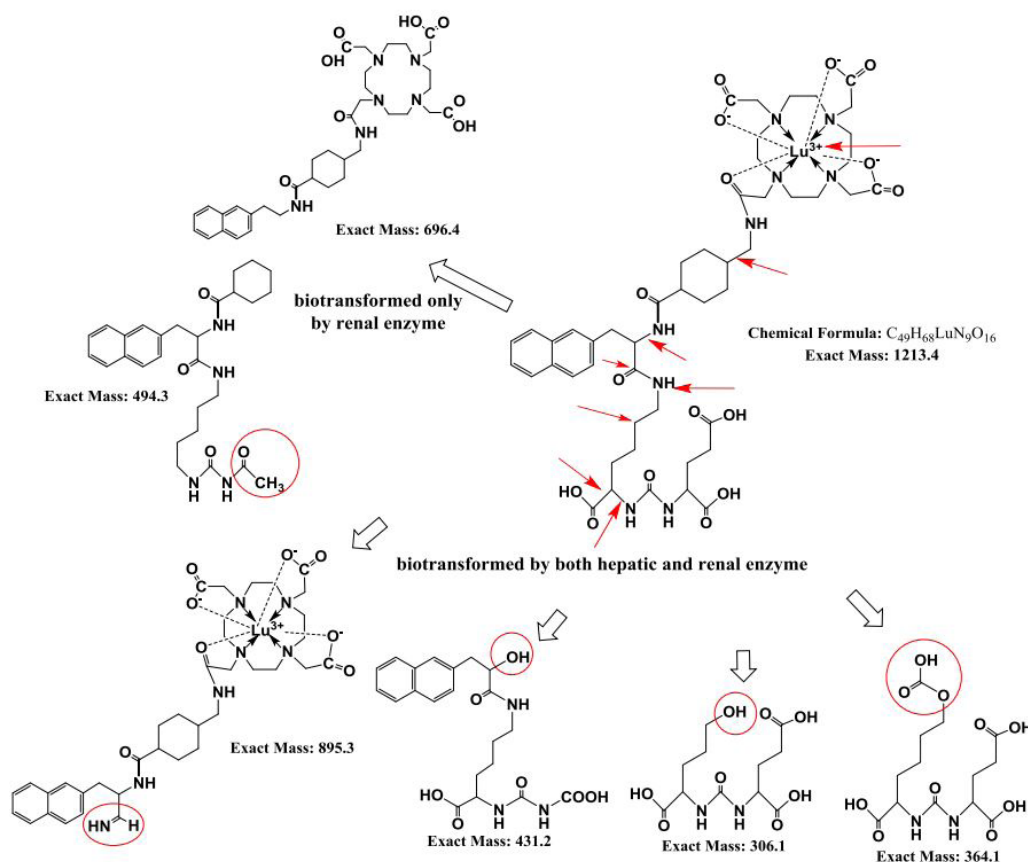

Figure 14: Metabolism study for Lu-PSMA-617 by rat liver microsomes and kidney homogenate.

Acknowledgments

Conflict of interest

The authors declare that they have no conflict of interest.

References

1. Siegel RL, Miller KD, Jemal A (2017) Cancer statistics. J Clin 67: 7.

2. Benesova M, Bauder-Wust U, Schafer M, (2016) Linker modification strategies to control the prostate-specific membrane antigen (PSMA)-targeting and pharmacokinetic properties of DOTA-conjugated PSMA inhibitors. J. Med. Chem. 59: 1761.

3. Osborne J, Deh K, Anand A, Bander N, Tagawa S (2013) Prostate specific membrane antigen-based diagnostics in Prostate cancer: A comprehensive perspective. Page: 448, Ed. Tewari A. Springer.

4. Wirtz M, Schmidt A, Schottelius M, Robu S, Gunter T, et al. (2018) Synthesis and in vitro and in vivo evaluation of urea-based PSMA inhibitors with increased lipophilicity EJNMMI Res 8: 84.

5. Ceci F, Fanti S (2019) PSMA-PET/CT imaging in prostate cancer: why and when. Clin. Transl. Imaging 7: 377.

6. Kim Y, Kim Y (2018) Therapeutic responses and survival effects of ^{177}Lu-PSMA-617 radioligand therapy in metastatic castrate-resistant prostate cancer. Clin. Nucl. Med. 43: 728.

7. Cardinale J, Schäfer M, Beneˇsová M (2017) Preclinical evaluation of ^{18}F-PSMA-1007, a new prostate-specific membrane antigen ligand for prostate cancer imaging. J. Nucl. Med. 58: 425.

8. Benešová M, Schäfer M, Bauder-Wüst U, Afshar-Oromieh A, Kratochwil C, et al. (2015) Preclinical Evaluation of a Tailor-Made DOTA-Conjugated PSMA inhibitor with optimized linker moiety for imaging and endoradiotherapy of prostate cancer. J Nucl Med 56: 914.

9. Kratochwil C, Giesel FL, Eder M, Afshar-Oromieh A, Benešová M, et al. (2015) [^{177}Lu]Lutetium-labelled PSMA ligand-induced remission in a patient with metastatic prostate cancer. Eur. J. Nucl. Med. Mol. Imaging 42: 987.

10. Khreish F, Ebert N, Ries M, et al. (2020) [225]Ac-PSMA-617/^{177}Lu-PSMA-617 tandem therapy of metastatic castration-resistant prostate cancer: pilot experience" Eur. J. Nucl. Med. Mol. Imaging 47: 721.

11. Cui C, Hanyu M, Haton A (2017) Synthesis and evaluation of [^{64}Cu] PSMA-617 targeted for prostate- specific membrane antigen in prostate cancer. Am. J. Nucl. Med. Mol. Imaging 7: 40.

12. Liu C, Liu T, Zhang N (2018) ^{68}Ga-PSMA-617 PET/CT: a promising new technique for predicting risk stratification and metastatic risk of prostate cancer patients. Eur. J. Nucl. Med. Mol. Imaging 45: 1852.

13. Eiber M, Fendler W, Rowe S (2017) Prostate-specific membrane antigen ligands for imaging and therapy" J Nucl Med. 58: 67S.

14. Weineisen M, Schottelius M, Simecek J (2015) [68]Ga- and ^{177}Lu-Labeled PSMA I&T: Optimization of a PSMA- targeted theranostic concept and first proof-of-concept human studies. J Nucl Med 56: 1169.

15. Hofman MS, Violet J, Hicks RJ (2018) [^{177}Lu]-PSMA-617 Radionuclide Treatment in Patients with Metastatic Castration-Resistant Prostate Cancer (LuPSMA Trial): A Single-Centre, Single-Arm, Phase 2 Study. Lancet Oncol. 19: 825.

16. Low P (2021) "[177]Lu-PSMA-617".

17. Dash A, Pillai MRA, Knapp FF (2015) Production of ^{177}Lu for targeted radionuclide therapy: available options. Nucl. Med. Mol. Imaging 49: 85.

18. Emmett L, Willowson K, Violet J, Shin J (2017) Lutetium-177 PSMA radionuclide therapy for men with prostate cancer: a review of the current literature and discussion of practical aspects of therapy. J. Med. Radiat. Sci. 64: 52.

19. Pilaniya K, Chandrawanshi HK, Pilaniya U, Manchandani P, Jain P, et al. (2010) Recent trends in the impurity profile of pharmaceuticals. J Adv Pharm Technol Res 1: 302.

20. "Mammalian liver microsomes" guidelines for use, TF000017 Rev 1.0. Issued by BD Biosciences.

21. Kaplan MM, Utiger RD (1978) Iodothyronine metabolism in rat liver homogenates. J Clin Invest 61: 459.

22. Stringer JL (2017) Chapter 5: Drug Metabolism and Renal Elimination in Basic Concepts in Pharmacology: What You Need to Know for Each Drug Class, 5th ed. McGraw Hil.

23. BD Gentest™, Tissue Fractions, Reagents for Drug Metabolism catalog.

24.   Lutetium: radii of atoms and ions, https://www.webelements.com/lutetium/atom_sizes.html accessed on July 16, 2020.

25.   Le J (2020) Drug Elimination.

26.   Knights KM, Rowland A, Miners JO (2013) Renal drug metabolism in humans: the potential for drug–endobiotic interactions involving cytochrome P450 (CYP) and UDP glucuronosyltransferase (UGT). Br.J. Clin. Pharmacol. 76: 587.

27.   Anders MW (1980) Metabolism of drugs by the kidney. Kidney Int. 18: 636.